



*Dedicated to the memory of
Academician Bogdan C. Simionescu (1948–2024)*

COORDINATION POLYMERS CONSTRUCTED FROM BINUCLEAR COPPER(II) CARBOHYDRAZONE NODES AND BIS(4-PYRIDYL) SPACERS^{*,**}

Natalia TALMACI,^a Teodora MOCANU,^b Sergiu SHOVA,^c Mihai RĂDUCĂ,^{d,e}
Diana DRAGANCEA^{d,*} and Marius ANDRUH^{d,e}

^a Institute of Chemistry, Academiei 3 Str., MD Chisinau, Republic of Moldova

^b Ilie Murgulescu Institute of Physical Chemistry, 202 Splaiul Independentei, 060021 Bucharest, Roumania

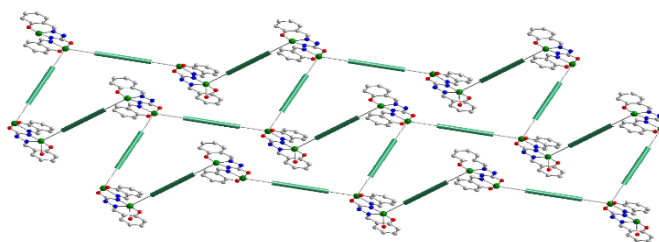
^c “Petru Poni” Institute of Macromolecular Chemistry of the Roumanian Academy,
Aleea Grigore Ghica Vodă 41-A, RO-700487 Iasi, Roumania

^d “C. D. Nenitzescu” Institute of Organic and Supramolecular Chemistry of the Romanian Academy,
Splaiul Independentei 202B, Bucharest, Roumania

^e Faculty of Chemistry, University of Bucharest, 4–12 Regina Elisabeta Blvd., 030018 Bucharest, Roumania

Received May 8, 2025

The condensation reaction between salicylaldehyde and carbohydrazone generates the 1,5-bis(2-hydroxybenzaldehyde) carbohydrazone (H₄L) Schiff base, which, upon reaction with copper(II) salts and *exo*-dentate ligands, 4,4'-dipyridyl (bipy) or 1,2-bis(4-pyridyl)ethane (bpyeta), leads to polymeric species ¹_∞[[Cu₂(HL)(H₂O)(NO₃)](μ-bipy)]·DMF (**1**), ¹_∞[[Cu₂(HL)(H₂O)(NO₃)](μ-bpyeta)]·DMF·H₂O (**2**), and ²_∞[[Cu₄(HL)₂(H₂O)](μ-bpyeta)₃](ClO₄)₂·1.5DMF·1.5H₂O (**3**). Compounds **1-3** have been characterized by spectroscopic methods and single crystal X-ray diffraction.



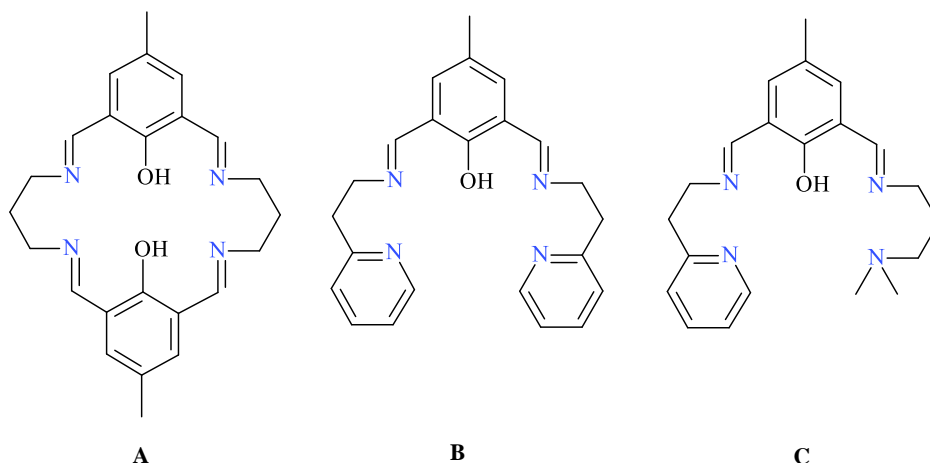
INTRODUCTION

The synthetic strategy based on Robson-type macrocyclic multidentate ligands obtained by the 2+2 template Schiff condensation of 2,6-diformyl-4-methylphenol with diamines (*e.g.* 1,3-diaminopropane) (Scheme 1A) allowed to synthesize

a wide range of binuclear complexes with relevance in bioinorganic chemistry, magnetochemistry, and catalysis.^{1,2} End-off binucleating acyclic ligands, obtained by a 1+2 condensation between the keto-precursor and the amine can be either symmetric (Scheme 1B) or dissymmetric, with two different compartments (Scheme 1C).^{3–6}

* Corresponding author: ddragancea@gmail.com

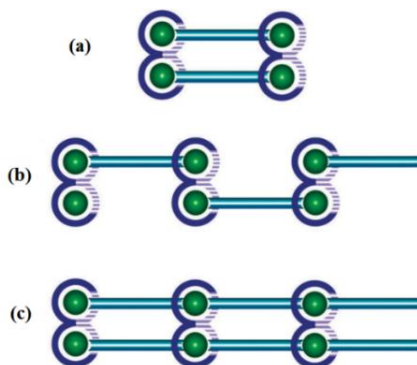
**Supplementary information on <https://www.icf.ro/rrech/> or <https://revroum.lew.ro>



Scheme 1 – Compartmental Schiff-base ligands.

Such binuclear complexes can be employed as nodes for the construction of coordination polymers using appropriate *exo*-dentate (divergent) ligands as spacers. In most cases, the coordination polymers assembled from these binuclear nodes, are mono-dimensional. For a 1 : 1 molar ratio between the binuclear complex and the *exo*-dentate ligand, two

types of polynuclear complexes can be assembled: discrete (tetranuclear rectangles – Scheme 2a), and 1D coordination polymers (Scheme 2b). 1D coordination polymers with a railroad topology are obtained when the molar ratio between the two components (dinuclear tecton and spacer) is 1 : 2 (Scheme 2c).

Scheme 2 – Molecular rectangles and coordination polymers constructed from binuclear precursors.⁵

Alcoxo-bridged binuclear Cu(II) species incorporating aminoalcohols, acted as nodes in the design of framework polymers with various dimensionalities and architectures, when neutral (*e.g.* bis(4-pyridyl) derivatives) or anionic divergent ligands (*e.g.* polycarboxylato anions, polycyanido-metallates) were employed as spacers.^{7,8}

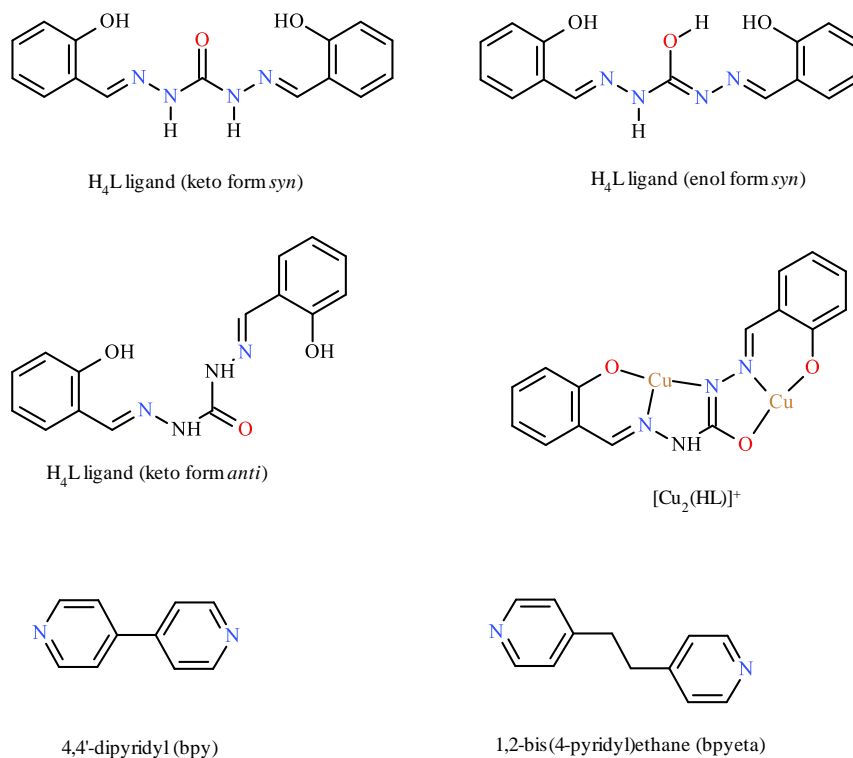
The ligand 1,5-bis(2-hydroxybenzaldehyde) carbohydrazone (HL), that can be easily obtained *via* the condensation reaction of carbohydrazone with 2-hydroxybenzaldehyde, proved its versatile coordination ability towards both *d*-^{9–19} and *f*-block^{20–23} metal ions. Usually, it behaves as a multidentate ligand and the reported structures vary from mononuclear,^{9,10} to dinuclear,^{11–16,20}

tetranuclear,^{15–17,21} and hexanuclear²² complexes. Unprecedented hexadecanuclear Gd^{III} and Dy^{III} complexes, with 1,5-bis(2-hydroxybenzaldehyde) carbohydrazone as chelating and bridging ligand, show a structural motif resembling naturally occurring minerals, such as brucite and hydrotalcite.²³ Additionally, the ability of the phenoxide group to bind more than one center, and to form polynuclear complexes is also known.^{16–19}

The use of symmetric ligands based on carbohydrazone and 2-hydroxybenzaldehyde for this purpose presents several advantages: (i) these molecules present an extremely versatile coordination behavior towards metal ions because they can act as mono-, di- and trianionic ligands,

due to the keto-enolic tautomerism; (ii) these molecules usually act as planar, bis-tridentate chelating ligands, coordinating through two sets of ONO and ONN donor atoms, forming binuclear

complexes (Scheme 3). The weakly coordinated anions or solvent molecules can be easily replaced by spacer ligands leading to coordination polymers or to high nuclearity aggregates.



Scheme 3 – H_4L and its binding modes to copper(II) ions and the bis(4-pyridyl) bridging ligands used in this work.

We report herein the new 1D and 2D coordination polymers, which are constructed from binuclear nodes, generated by a Schiff base carbohydrazone and 4,4'-dipyridyl, and bis(4-pyridyl)ethane as spacers.

RESULTS AND DISCUSSION

The proligand, 1,5-bis(2-hydroxybenzaldehyde) carbohydrazone (H_4L), was prepared by heating 2-hydroxybenzaldehyde with carbohydrazide in 2:1 molar ratio in an ethanol/water solution. The reaction of $Cu(NO_3)_2 \cdot 3H_2O$ with H_4L and 4,4'-dipyridyl (bipy) in DMF in 2:1:4 ratio, at room temperature, produced green crystals of $^1_\infty\{[Cu_2(HL)(H_2O)(NO_3)](\mu-bipy)\} \cdot DMF$ (**1**), which were separated after 2 weeks in 37% yield. If 1,2-bis(4-pyridyl)ethane (bpyeta) is used as a linker, the reaction mixture generates green crystals with the composition $^1_\infty\{[Cu_2(HL)(H_2O)(NO_3)](\mu-bpyeta)\} \cdot DMF \cdot H_2O$ (**2**), which were isolated in 56% yield. Starting from $Cu(ClO_4)_2 \cdot 6H_2O$,

H_4L , and bpyeta in 2:1:4 molar ratio in DMF, green crystals of $^2_\infty\{[Cu_4(HL)_2(H_2O)](\mu-bpyeta)_3\}(ClO_4)_2 \cdot 1.5DMF \cdot 1.5H_2O$ (**3**) were obtained and separated after 2 days in 37% yield. The crystalline phase purity of the samples **1–3** was confirmed by the good agreement between the PXRD patterns and the ones simulated using single-crystal diffraction data (Figs. S1–3).

The analysis of the IR spectra of compounds **1–3** (Figs. S4–6) shows that the $\nu(C=O)$ band observed in the ligand spectrum at 1680 cm^{-1} is shifted to lower frequencies in the spectra of the complexes: 1654 (**1**), 1655 (**2**), 1657 cm^{-1} (**3**). The appearance of the $\nu(C=O)$ stretching vibration band suggests the absence of enolization, and the delocalization within the $-N-C=O$ moiety in the coordinated ligand. The evaluation of the N–C and C=O bond lengths in the $-N-C=O$ fragment, according to the X-Ray data, suggests that the C–O bond is lengthened, and one of the C–N bonds is shortened, which indicates the electronic delocalization in this fragment. The bands at 1594 (**1**), 1599 (**2**), and 1602 cm^{-1} (**3**) witness the coordination of the azomethine nitrogen atom to the Cu(II) ion. The

weak bands at ca. 3200–3225 cm^{-1} are due to the presence of a N–H bond in **1–3**, and confirm the presence of an amide hydrogen atom. The weak bands at 3050 (**1**), 3053 (**2**), and 2988 (**3**) cm^{-1} , and the strong bands at 749 (**1**), 753 (**2**), 748 (**3**) cm^{-1} are due to aromatic C–H vibrations. In addition, the following bands were assigned to the coordinated nitrate anion: 1308 cm^{-1} (**1**) and 1298 cm^{-1} (**2**). The bands located at 1078 and 620 cm^{-1} are assigned to the perchlorate anion in **3**.²⁴

Thus, the IR spectroscopy and crystallographic data support the elimination of the amidic hydrogen without enolization through the –N–C=O group, a phenomenon observed in copper, manganese and vanadium complexes.¹⁹

The new coordination compounds, **1–3**, are sparingly soluble in common organic solvents like methanol, DMF and DMSO. The ESI-MS spectra (in the positive-ion mode) for complexes **1** and **3** have been recorded in DMSO and are presented in Figs. S7–8 (Supplementary material). Intense peaks at m/z 421 and 843 are assigned to $[\{\text{Cu}_2(\text{HL})\}]^+$ and $[\{\text{Cu}_2(\text{HL})\}_2\text{H}^+]^+$, respectively, whose experimental isotopic patterns fit the calculated values for the two ions. Most likely in DMSO solution the fragmentation of the chains into more stable binuclear fragments occurs.

Crystal structures

$[\{\text{Cu}_2(\text{HL})(\text{H}_2\text{O})(\text{NO}_3)\}(\mu\text{-bipy})]\cdot\text{DMF}$ (**1**)

A view of the asymmetric unit in the crystal **1** is shown in Fig. 1, and selected bond distances and

bond angles are collected in Table 1. The asymmetric unit of **1** consists of a dicopper(II) unit, $\{\text{Cu}_2(\text{HL})\}$, formed by the triply deprotonated ligand, HL^{3-} , coordinated to two copper ions through two donor sets (ONN and ONO), two halves from two 4,4'-dipyridyl spacers, a nitrate ligand, one aqua ligand, and one crystallization DMF molecule (Fig. 1). Two crystallographically independent copper(II) atoms are pentacoordinated with a square-pyramidal geometry, the values of the τ_5 parameters²⁵ being 0.18 for Cu1 and 0.10 for Cu2, and are bridged by the N–N diazine fragment of the hexadentate ligand with a Cu1...Cu2 separation of 4.8121(4) Å. The Cu–N–N–Cu torsional angle is 168.8(1)°. The Cu1 and Cu2 atoms accommodated into the ONN and ONO ligand pockets, respectively, are bridged by one 4,4'-dipyridyl molecule. The fifth positions are occupied by the semicoordinated nitrate anion (Cu1) and by the aqua ligand (Cu2). The C8–O2 bond length increases from 1.217(3) Å in the copper-free ligand to 1.266(2) Å in **1**, while the C–N bond shortens from 1.375(2) to 1.332(3) Å, indicating that the ligand adopts the enolate form. The 4,4'-bipy molecules assemble the dinuclear species into a 1D polymeric structure with a zig-zag chain motif (Fig. 2). The interaction between the nitrate oxygen atoms of one chain and the NH groups arising from neighboring chains describes a supramolecular grid-like hydrogen-bonded network ($\text{N2}\cdots\text{O6}^a = 2.802$ Å, $a = 1-x, 1-y, 1-z$) (Fig. 3).

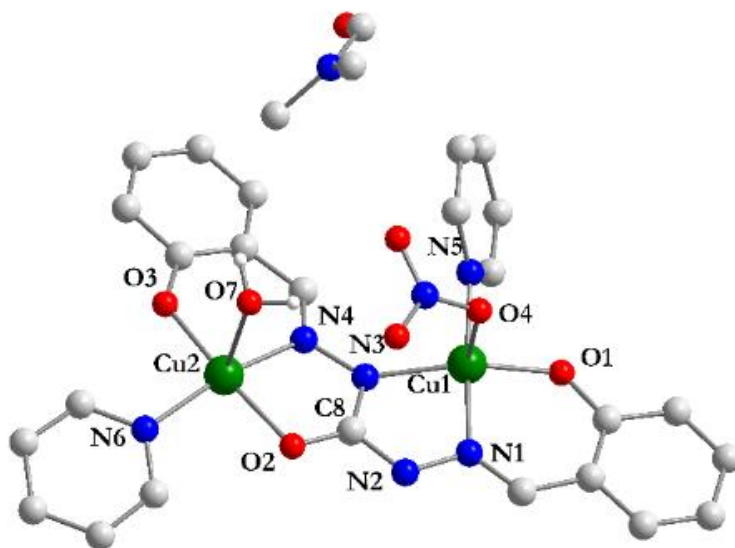


Fig. 1 – The asymmetric unit $[\text{Cu}_2(\text{HL})(\mu\text{-bpy})(\text{H}_2\text{O})(\text{NO}_3)]$ and crystallization DMF molecule in **1**.

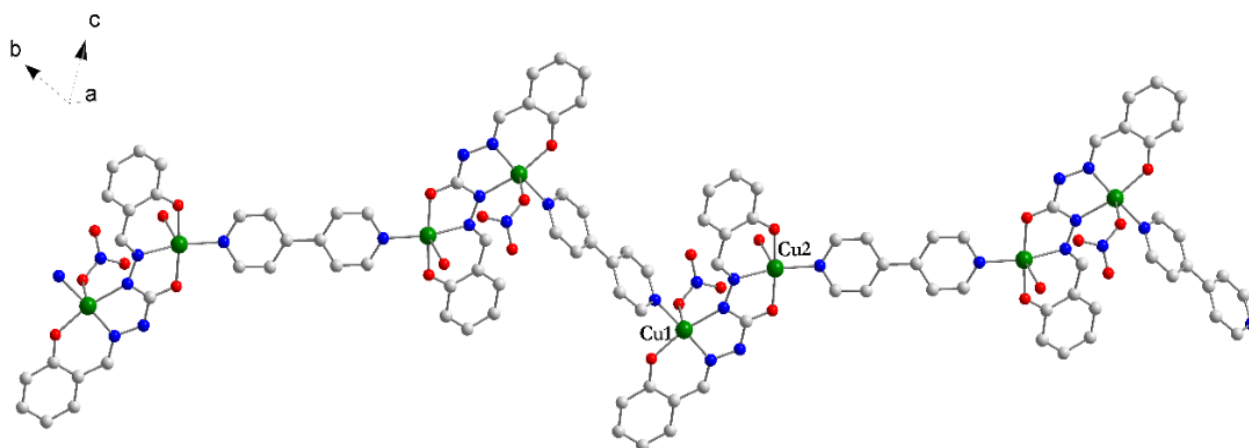


Fig. 2 – View of the 1D polymeric structure with a zig-zag chain motif in **1**.

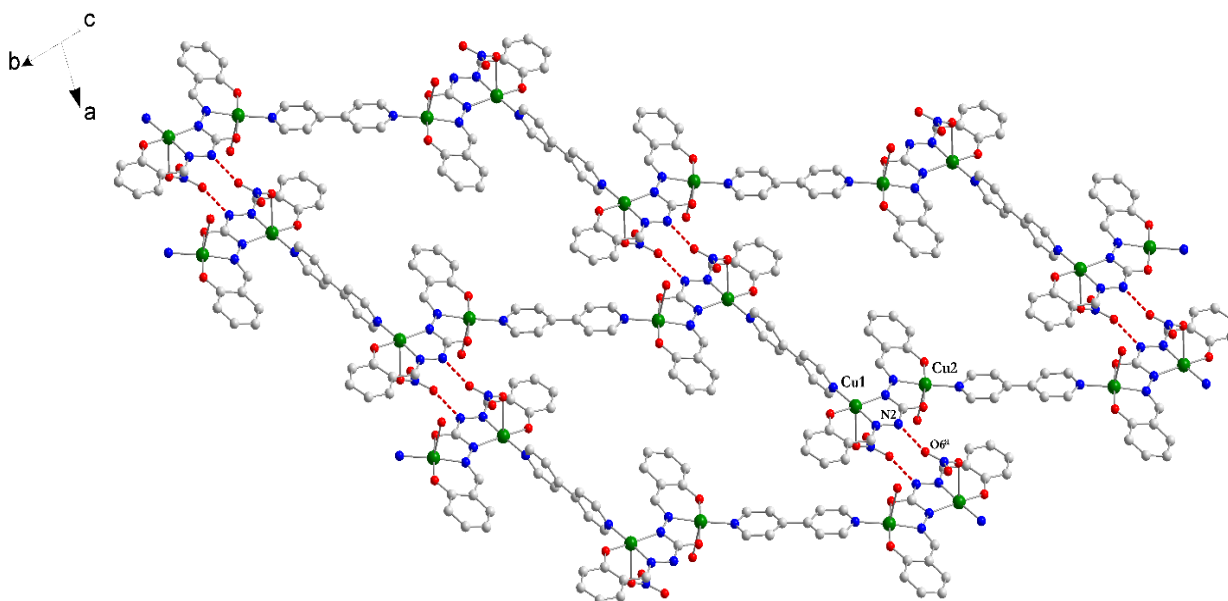


Fig. 3 – The supramolecular grid-like hydrogen-bonded network in **1** (Symmetry code: $a = 1-x, 1-y, 1-z$).

$1/2$ $[(Cu_2(HL)(H_2O)(NO_3))(\mu-bipyeta)] \cdot DMF \cdot H_2O$ (**2**)

Compounds **1** and **2** are isostructural, except the presence of an additional crystallization water molecule. The crystal structure analysis reveals that in compound **2** the water molecule and the nitrogen ion are interchanged compared to the asymmetric unit in complex **1** (Figs. 4, 5). The coordination sphere of the Cu(II) ions located into the ONN and ONO donor sets is completed by an aqua ligand and a nitrate anion, respectively, in contrast to the crystal structure of **1**. Selected bond distances and bond angles are gathered in Table 1. The Cu1 and

Cu2 atoms adopt a square-pyramidal geometry ($\tau_5 = 0.28$ and 0.05 , respectively), and are bound to ONN and ONO donors of the HL³⁻ ligand, a nitrogen atom from the bipyeta spacer and an oxygen atom belonging to either a water molecule or a nitrate anion, respectively. An extensive network of hydrogen bonds, involving hydrazine nitrogen atoms, nitrate anions, and water and DMF molecules in the outer sphere, unite the crystal components in **2**, resulting into a supramolecular layer similar to compound **1** ($N2 \cdots O6^a = 2.864 \text{ \AA}$, $a = -x, 1-y, 1-z$) (Fig. 6).

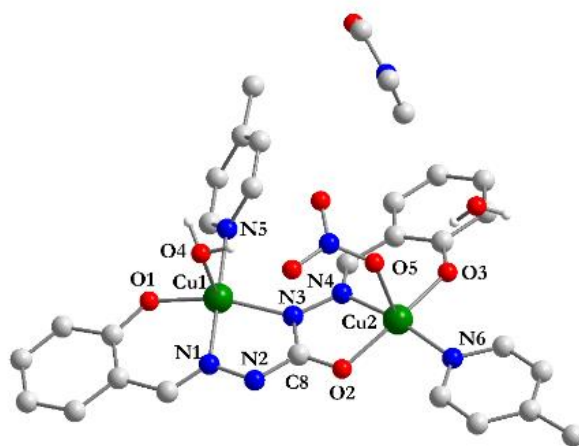


Fig. 4 – The asymmetric unit $[\text{Cu}_2(\text{HL})(\text{bpyeta})(\text{H}_2\text{O})(\text{NO}_3)]$ in **2**.

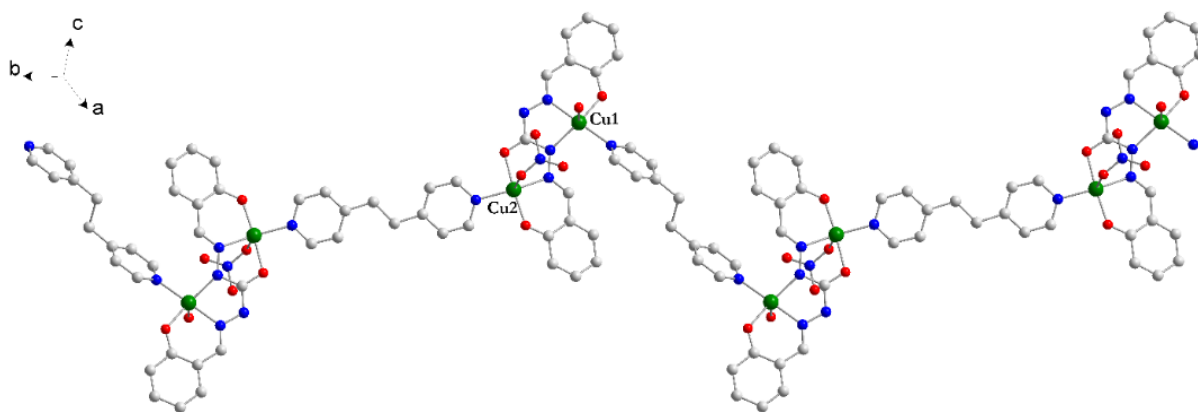


Fig. 5 – View of the 1D polymeric structure with a zig-zag chain motif in **2**.

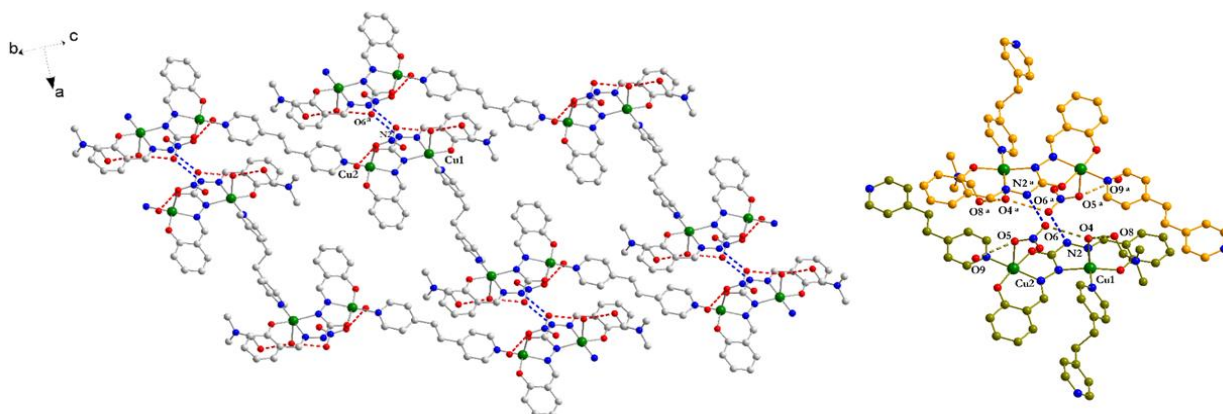


Fig. 6 – The supramolecular hydrogen-bonded network in **2** (Symmetry code: $a = -x, 1-y, 1-z$) and its fragment showing involved oxygen and nitrogen atoms.

$2_{\infty}[\{\text{Cu}_4(\text{HL})_2(\text{H}_2\text{O})\}\{\mu\text{-bpyeta}\}_3](\text{ClO}_4)_2 \cdot 1.5\text{DMF} \cdot 1.5\text{H}_2\text{O}$ (**3**)

The analysis of the asymmetric unit in **3** revealed that it contains four Cu(II) atoms connected by bpyeta and azine bridges, two ClO_4^- ions, and

solvent molecules (1.5 DMF and 1.5 H_2O) (Fig. 7). The four crystallographic non-equivalent Cu(II) ions are grouped in pairs by the two HL^{3-} ligand molecules with Cu1 and Cu4 placed in ONN donor sets and Cu2 and Cu3 in the ONO ones.

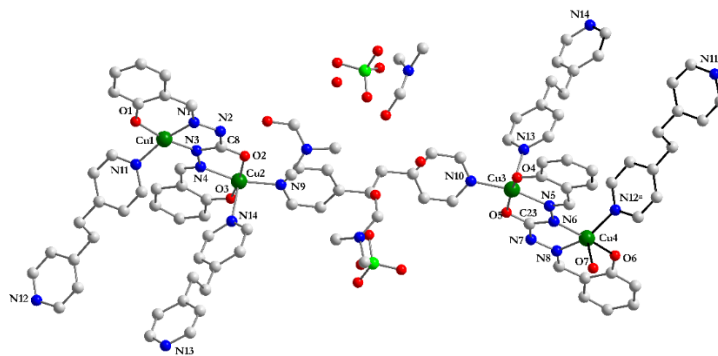


Fig. 7 – The asymmetric unit $\{[\text{Cu}_4(\text{HL})_2(\mu\text{-bpyeta})_3(\text{H}_2\text{O})]^{2+}\}$ in **3**. (Symmetry code: $a = x, -1+y, 1+z$).

The three non-equivalent bpyeta molecules play different roles: one (N9–N10) connects the two pairs by coordinating to Cu2 and Cu3, the second one (N11–N12) is bonded to Cu1 and Cu4, linking the

tetranuclear units into linear chains, and the third one (N13–N14) is oriented perpendicular to the chains and extends the structure into the second dimension, generating a cationic brick-wall type layer (Fig. 8).

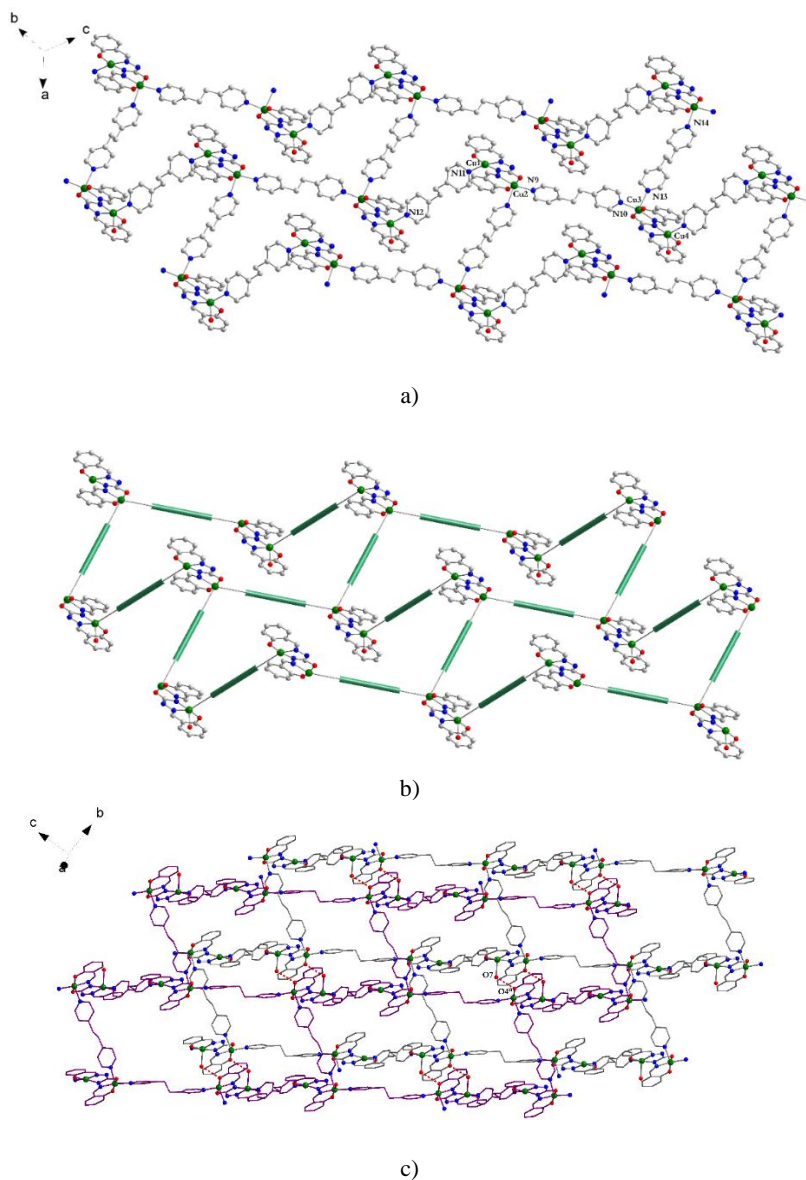


Fig. 8 – a) View of the 2D brick wall type layer in **3**; b) Simplified view by replacing the spacers by green rods; c) perspective view of two layers connected through H-bonds (Symmetry code: $a = 1-x, -y, 1-z$).

Table 1
Selected bond distances (Å) and angles (°) for 1–3

1		2		3	
Cu1–O1	1.893(2)	Cu1–O1	1.8919(19)	Cu1–O1	1.881(3)
Cu1–O4	2.512(2)	Cu1–O7w	2.423(2)	Cu1–N1	1.939(3)
Cu1–N1	1.950(3)	Cu1–N1	1.955(2)	Cu1–N3	1.969(3)
Cu1–N3	2.003(2)	Cu1–N3	1.990(2)	Cu1–N11	1.978(3)
Cu1–N6	2.006(3)	Cu1–N5	2.004(2)	Cu2–O2	1.997(3)
Cu2–O2	1.966(2)	Cu2–O2	1.9683(18)	Cu2–O3	1.904(3)
Cu2–O3	1.878(2)	Cu2–O3	1.8861(19)	Cu2–N4	1.961(3)
Cu2–O7w	2.472(3)	Cu2–O4	2.507	Cu2–N9	2.011(3)
Cu2–N4	1.947(2)	Cu2–N4	1.941(2)	Cu2–N14 ^a	2.270(3)
Cu2–N5	2.008(2)	Cu2–N6	1.986(2)	Cu3–O4	1.922(3)
N2–C8	1.350(3)	N2–C8	1.347(3)	Cu3–O5	1.986(3)
C8–O2	1.266(2)	C8–O2	1.268(3)	Cu3–N5	1.955(3)
C8–N3	1.333(3)	C8–N3	1.340(3)	Cu3–N10	1.993(3)
O1Cu1N1	91.35(7)	O1Cu1N1	91.95(9)	Cu3–N13	2.263(3)
N1Cu1N3	80.52(7)	N1Cu1N3	80.21(8)	Cu4–O6	1.907(3)
N3Cu1N5	102.33(7)	N3Cu1N5	100.10(8)	Cu4–O7	2.210(3)
O1Cu1N5	85.88(7)	O1Cu1N5	88.33(9)	Cu4–N6	1.988(3)
N1Cu1O4	85.80(8)	N1Cu1O4	87.38(8)	Cu4–N8	1.968(3)
O1Cu1N3	166.34(8)	O1Cu1N3	161.00(11)	Cu4–N12 ^b	2.026(3)
O1Cu1O4	100.22(8)	O1Cu1O4	99.23(10)	N2–C8	1.351(5)
N3Cu1O4	90.19(8)	N3Cu1O4	97.67(8)	C8–O2	1.265(5)
N5Cu1O4	93.97(8)	N5Cu1O4	90.65(8)	C8–N3	1.347(5)
N1Cu1N5	177.13(7)	N1Cu1N5	178.03(9)	N7–C23	1.345(6)
O2Cu2N6	92.62(7)	O2Cu2N6	93.20(8)	C23–O5	1.262(5)
O2Cu2O7	93.07(9)	O2Cu2O5	89.39(9)	C23–N6	1.349(5)
O3Cu2O2	174.59(6)	O3Cu2O2	173.25(8)	O1Cu1N1	93.31(13)
O3Cu2N4	93.65(7)	O3Cu2N4	93.33(8)	N1Cu1N3	81.38(13)
O3Cu2N6	92.57(7)	O3Cu2N6	91.94(9)	N3Cu1N11	97.70(13)
O3Cu2O7	87.73(10)	O4Cu2O5	94.69(10)	O1Cu1N11	89.57(13)
N4Cu2O2	80.98(6)	N4Cu2O2	80.96(8)	O1Cu1N3	169.87(13)
N4Cu2N6	168.36(8)	N4Cu2N6	170.12(10)	N1Cu1N11	165.66(14)
N4Cu2O7	92.47(9)	N4Cu2O5	94.78(9)	O2Cu2N4	80.44(12)
N6Cu2O7	97.60(9)	N6Cu2O5	93.11(9)	O3Cu2N4	92.98(13)
				O3Cu2N9	93.53(13)
				O3Cu2N14 ^a	94.45(13)
				N4Cu2N14 ^a	95.30(13)
				O3Cu2O2	168.24(13)
				N4Cu2N9	164.19(14)
				O4Cu3N5	93.45(13)
				O5Cu3N5	81.04(13)
				O5Cu3N10	90.91(13)
				O4Cu3N10	91.79(13)
				N5Cu3N13	93.98(13)
				N10Cu3N13	95.83(13)
				O4Cu3O5	163.58(13)
				N5Cu3N10	167.83(14)
				O6Cu4N8	91.90(14)
				N6Cu4N8	80.54(14)
				N6Cu4N12 ^b	96.19(13)
				O6Cu4N12 ^b	89.90(13)
				N6Cu4O7	91.10(13)
				O6Cu4O7	93.06(14)
				O6Cu4N6	172.30(13)
				O7Cu4N12 ^b	95.06(15)
				O7Cu4N8	111.48(14)

a = x, y, –1+z; b = x, –1+y, 1+z

The Cu1 atoms are four coordinated, with a pyridyl moiety occupying the fourth position. Cu2 and Cu3 show a square pyramidal stereochemistry

($\tau_5 = 0.08$ and 0.07 , respectively), featuring similar coordination spheres: the basal plane is formed by ONN donor atoms of HL³⁻ ligand and a nitrogen

atom belonging to N9–N11 bpyeta molecule. In the apical position is placed a second spacer molecule (N13–N14). In the case of Cu4 atoms, the square pyramidal geometry is defined by ONN donor group, a pyridyl nitrogen atom and an aqua oxygen atom in the fifth coordination site ($\tau_5 = 0.32$). Two adjacent layers stacked in an AB fashion are interconnected through H-bonds established

between coordinated water molecules and phenoxido oxygen atoms bonded to Cu3 ions ($O7 \cdots O4^a = 2.761 \text{ \AA}$, $a = 1-x, -y, 1-z$).

The UV-Vis spectra of compounds **1–3** are shown in Fig. 9. The three complexes show a large band between 200 and 1000 nm, being a convolution of ligand-to-metal charge transfer,²⁶ and d-d bands.

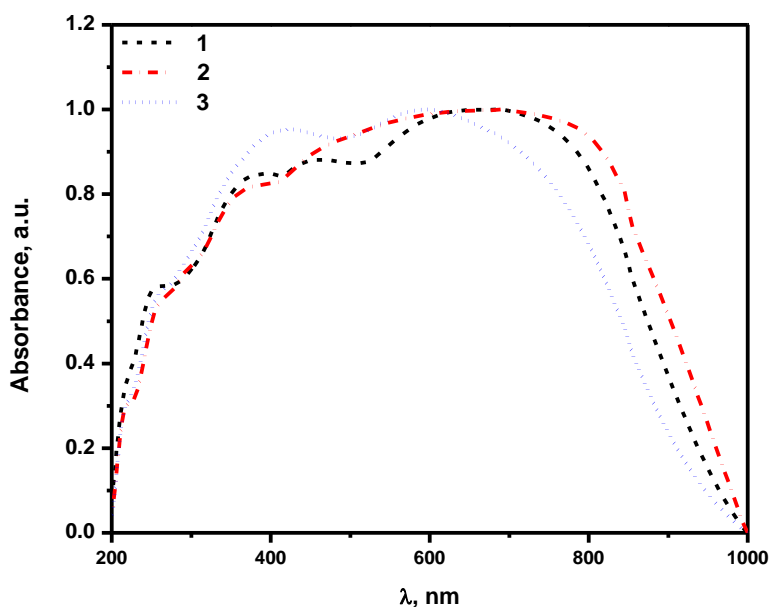


Fig. 9 – Diffuse reflectance spectra of compounds **1–3**.

EXPERIMENTAL

All the used chemicals were purchased from commercial sources and used without further purification. 1,5-Bis(2-hydroxybenzaldehyde) carbohydrazone (H_4L) was prepared by the procedure reported previously.¹⁶

Syntheses of complexes

$^1_{\infty}[\{Cu_2(HL)(H_2O)(NO_3)\}(\mu\text{-bipy})] \cdot DMF$ (**1**)

A mixture of 1,5-bis(2-hydroxybenzaldehyde) carbohydrazone (H_4L) (0.030 g, 0.1 mmol), $Cu(NO_3)_2 \cdot 3H_2O$ (0.048 g, 0.2 mmol), and 4,4'-dipyridyl (0.062 g, 0.4 mmol), in DMF (10 mL) was stirred at room temperature for 2 h. The green solution was filtered and the filtrate was allowed to stand at room temperature for crystallization. After 7 days green crystals were filtered off, washed with ethanol and dried in air. Yield: 0.053g (37%). Selected IR bands (ν , cm^{-1}): 1601, 1494, 1469, 1413, 1385, 1336, 1309, 1201, 1113, 1012, 954, 755, 735, 586.

$^1_{\infty}[\{Cu_2(HL)(H_2O)(NO_3)\}(\mu\text{-bpyeta})] \cdot DMF \cdot H_2O$ (**2**)

Compound **2** was obtained by a similar procedure to **1**, except that 1,2-bis(4-pyridyl)ethane (0.073 g, 0.4 mmol) was used. After 48 h a clear green solution produced green crystals, which were filtered off, washed with ethanol and dried in air. Yield: 0.043 g (56%). Selected IR bands (ν , cm^{-1}): 3378, 3053, 1655, 1599, 1490, 1298, 1197, 1103, 960, 841, 753, 660.

$^2_{\infty}[\{Cu_4(HL)_2(H_2O)\}(\mu\text{-bpyeta})_3](ClO_4)_2 \cdot 1.5DMF \cdot 1.5H_2O$ (**3**)

Compound **3** was obtained by a similar procedure to **2**, except that $Cu(ClO_4)_2 \cdot 6H_2O$ (0.074 g, 0.2 mmol) was used. Yield: 0.036g (37%). Selected IR bands (ν , cm^{-1}): 3055, 1657, 1602, 1497, 1414, 1197, 1078, 819, 757, 620.

X-ray data collection and crystal structure refinement

X-ray diffraction measurements were performed on a Rigaku XtaLAB Synergy-S (**1–2**) and on a

XtaLAB Synergy, Dualflex (3) diffractometers operating with Mo-K α ($\lambda = 0.71073 \text{ \AA}$) and Cu-K α ($\lambda = 1.54184 \text{ \AA}$), respectively, microfocus sealed X-ray tube. The structure was solved by direct methods and refined by full-matrix least squares techniques based on F^2 . The non-H atoms were refined with anisotropic displacement parameters. Calculations were performed using SHELX-2014 or SHELX-2018 crystallographic software package.^{27–30} A summary of the crystallographic data and the structure refinement are given in Table S1. CCDC reference number: 2448971–2448973. The X-ray powder diffraction data were measured on a Proto AXRD benchtop using Cu-K α radiation with a wavelength of 1.54059 \AA in the range 5–35° (2 θ).

Physical Measurements

IR spectra were recorded on a Tensor 37 spectrophotometer in the 4000–400 cm^{-1} region. UV-Vis spectra were recorded on a JASCO V-670 spectrophotometer equipped with diffuse reflectance accessories, on MgO diluted samples from 200 to 1600 nm. For MS spectra Varian 310 – MS LC/MS/MS triple quadrupole mass spectrometer fitted with an electrospray ionization interface (ESI) was used. Air was used as drying gas at a pressure of 19 psi and temperature depending on the experiment. The nebulizing gas was nitrogen to 40 psi and the needle voltage had been established to the potential +5000 V for positive ionization. Thus, protonated molecular ion obtained was selected by the first quadrupole. Into the second quadrupole, the protonated molecular ion was fragmented by collision with an inert gas (Ar) to 1.5 mTorr pressure. Fragments were analyzed by the third quadrupole. Prior to these experiments it was performed the tuning of mass spectrometer using PPG both for positive and negative.

CONCLUSIONS

In the literature,^{31–33} there are only a few reports of Cu(II) compounds with tridentate Schiff bases, which served as precursors for obtaining polymers with linear bis(4-pyridyl) derivatives as spacers. We have shown herein that dinuclear Cu(II) complexes with a carbohydrazone ligand can be efficiently employed as building-blocks in metallosupramolecular chemistry and crystal engineering in order to construct 1D and 2D coordination polymers. According to the X-ray crystallography in

complexes 1–3 the ligand acts as triply deprotonated base and adopts the *anti* configuration with two different metal-binding-sites. 1D and 2D coordination polymers were obtained, with the binuclear nodes connected by one or two spacers. The architecture and stability of the overall supramolecular networks is driven by non-covalent bonds.

REFERENCES

1. P. A. Vigato and S. Tamburini, *Coord. Chem. Rev.*, **2008**, 252, 1871–1995.
2. P. A. Vigato, V. Peruzzo and S. Tamburini, *Coord. Chem. Rev.*, **2012**, 256, 953–1114.
3. M. Andruh, *Pure Appl. Chem.*, **2005**, 77, 1685–1706.
4. M. Andruh, *Chem. Commun.*, **2007**, 2565–2577.
5. G. Marinescu, G. Marin, A. M. Madalan, A. Vezeanu, C. Tiseanu and M. Andruh, *Crystal Growth Des.*, **2010**, 10, 2096–2103.
6. M. Andruh, *CHIMIA*, **2013**, 67, 383–387.
7. G. Marin, M. Andruh, A. M. Madalan, A. J. Blake, C. Wilson, N. R. Champness and M. Schröder, *Cryst. Growth Des.*, **2008**, 8, 964–975.
8. T. Mocanu, V. Tudor and M. Andruh, *CrystEngComm*, **2017**, 19, 3538–3552.
9. M. Sutradhar, T. Roy Barman and E. Rentschler, *Inorg. Chem. Commun.*, **2014**, 39, 140–143.
10. S. U. Parsekar, P. Velankanni, S. Sridhar, P. Haldar, N. A. Mate, A. Banerjee, P. K. Sudhadevi Antharjanamkoley, A. P. Koley and M. Kumar, *Dalton Trans.*, **2020**, 49, 2947–2965.
11. C. Bustos, O. Burckhardt, R. Schreiber, D. Carrillo, A. M. Arif, A. H. Cowley and C. M. Nunn, *Inorg. Chem.*, **1990**, 29, 3996–4001.
12. A. Maurya and C. Haldar, *Appl. Organomet. Chem.*, **2021**, 35, e6203.
13. S. U. Parsekar, M. Singh, D. P. Mishra, P. K. S. Antharjanam, A. P. Koley and M. Kumar, *J. Biol. Inorg. Chem.*, **2019**, 24, 343–363.
14. M. K. Koley, N. Duraipandy, M. S. Kiran, B. Varghese, P. T. Manoharan and A. P. Koley, *Inorg. Chim. Acta*, **2017**, 466, 538–550.
15. D. Dragancea, N. Talmaci, S. Shova, G. Novitchi, D. Darvasiová, P. Rapta, M. Breza, M. Galanski, J. Kožíšek, N. M. R. Martins, L. M. D. R. S. Martins, A. J. L. Pombeiro and V. B. Arion, *Inorg. Chem.*, **2016**, 55, 9187–9203.
16. D. Dragancea, S. Shova, É. A. Enyedy, M. Breza, P. Rapta, L. M. Carrella, E. Rentschler, A. Dobrov and V. B. Arion, *Polyhedron*, **2014**, 80, 180–192.
17. C. Zhang, X.-D. Ma, Z.-H. Chen, S.-H. Zhang and H. Hai, *J. Clust. Sci.*, **2017**, 28, 3241–3252.
18. E. Topić, J. Pisk, D. Agustin, M. Jendrlin, D. Cvijanović, V. Vrdoljak and M. Rubčić, *New J. Chem.*, **2020**, 44, 8085–8097.
19. R. Bikas, H. Hosseini-Monfared, M. Korabik, M. S. Krawczyk and T. Lis, *Polyhedron*, **2014**, 81, 282–289.
20. J.-Y. Wei, T.-J. Hsu, C.-W. Wang, C.-J. Kuo and P.-H. Lin, *Eur. J. Inorg. Chem.*, **2018**, 29, 3397–3401.
21. Y. Fang, X.-Q. Ji, J. Xiong, G. Li, F. Ma, H.-L. Sun, Y.-Q. Zhang and S. Gao, *Dalton Trans.*, **2018**, 47, 11636–11644.

22. R. J. Holmberg, C.-J. Kuo, B. Gabidullin, C.-W. Wang, R. Clérac, M. Murugesu and P. H. Lin, *Dalton Trans.*, **2016**, 45, 16769–16773.
23. P. Richardson, T.-J. Hsu, C.-J. Kuo, R. J. Holmberg, B. Gabidullin, M. Rouzières, R. Clérac, M. Murugesu and P.-H. Lin, *Dalton Trans.*, **2018**, 47, 12847–12851.
24. K. Nakamoto, "Infrared and Raman Spectra of Inorganic and Coordination Compounds", 4th edition, Wiley-Interscience, New York, 1986, 232–233.
25. A. W. Addison, T. N. Rao, J. Reedijk, J. van Rijn and G. C. Verschoor, *J. Chem. Soc., Dalton Trans.*, **1984**, 1349–1356.
26. A. B. P. Lever, "Inorganic Electronic Spectroscopy", Elsevier, Amsterdam, 1968, pp. 356–361.
27. CrysAlis RED, Version 1.171.34.76; Oxford Diffraction, Ltd., 2003.
28. G. M. Sheldrich, *Acta Cryst.*, **2015**, A71, 3–8.
29. G. M. Sheldrich, *Acta Cryst.*, **2015**, C71, 3–8.
30. O. V. Dolomanov, L. J. Bourhis, R. J. Gildea, J. A. K. Howard and H. Puschmann, *J. Appl. Cryst.*, **2009**, 42, 339–341.
31. S. Hazra, A. Karmakar, M. F. C. G. da Silva, E. Dlháň, R. Boča and A. J. L. Pombeiro, *Inorg. Chem. Commun.*, **2014**, 46, 113–117.
32. S. V. F. Beddoe, A. J. Fitzpatrick, J. R. Price, N. Mallo, J. E. Beves, G. G. Morgan, J. A. Kitchen and T. D. Keene, *Cryst. Growth Des.*, **2017**, 17, 6603–6612.
33. Yu. M. Chumakov, V. L. Tsapkov, P. A. Petrenko, L. G. Popovski, Yu. A. Simonov, G. Bocelli, B. Ya. Antosyak, A. O. Paraschivescu and A. P. Gulea, *Russ. J. Coord. Chem.*, **2009**, 35, 504–511.

